Metals **2013**, *3*, 69-76; doi:10.3390/met3010069

OPEN ACCESS

metals

ISSN 2075-4701

www.mdpi.com/journal/metals/

Article

Exchange Bias and Inverse Magnetocaloric Effect in Co and Mn Co-Doped Ni_2MnGa Shape Memory Alloy

Baomin Wang and Yong Liu *

School of Mechanical and Aerospace Engineering, Nanyang Technological University, 50 Nanyang Avenue, Singapore 639798, Singapore; E-Mail: wang0366@e.ntu.edu.sg

***** Author to whom correspondence should be addressed; E-Mail: mliuy@ntu.edu.sg; Tel./Fax: +65-67904951.

Received: 13 December 2012; in revised form: 8 January 2013 / Accepted: 17 January 2013 / Published: 25 January 2013

Abstract: Exchange bias effect observed in the $Ni_{1.68}Co_{0.32}Mn_{1.20}Ga_{0.80}$ alloy confirms the coexistence of antiferromagnetic and ferromagnetic phases in the martensite phase. A large inverse magnetocaloric effect has been observed within the martensitic transformation temperature range, which is originated from modified magnetic order through magnetic-field-induced phase transformation from partially antiferromagnetic martensite to ferromagnetic austenite. The magnetic entropy change is 16.2 J kg^{-1} K^{-1} at 232 K under ΔH = 60 kOe, with the net refrigerant capacity of 68 J kg^{-1}. These properties indicate Co and Mn co-doped Ni_2MnGa alloy is a multifunctional material potentially suitable for magnetic refrigeration and spintronics applications.

Keywords: shape memory alloy; exchange bias; inverse magnetocaloric effect; Ni-Mn-Ga; martensitic transformation

1. Introduction

Stoichiometric Ni_2MnGa is a full Heusler alloy that undergoes two separate transitions on cooling: (i) a magnetic transition (paramagnetic-ferromagnetic (FM) transition in the austenite) at T_c = 376 K, and (ii) a structural transition (martensitic transformation (MT) from austenite to martensite) at T_M = 202 K [1]. In both austenitic (below Curie temperature T_c) and martensitic states, the magnetic couplings are FM, giving rise to a small magnetization difference (ΔM) between austenite and martensite. A large magnetocaloric effect (MCE) has been observed when applying a magnetic field at

temperatures close to the MT [2–6]. By varying the composition, the transition temperature can be altered within a broad temperature range. The maximum MCE was obtained when structural and magnetic transition temperatures overlap each other ($T_M = T_c$) [3]. Furthermore, an extrinsic inverse MCE (IMCE, namely, positive ΔS_M) phenomenon has also been reported in several Ni-Mn-Ga alloys under application of low magnetic field, arising from the coupling between the martensitic and magnetic domains at the mesoscale [4], *i.e.*, magnetization change due to martensite reorientation associated with the high magnetic anisotropy. However, this process cannot result in a true ΔS_M since it is originated from the field dependent change of magnetic order parameter [7]. On the other hand, the intrinsic IMCE has been observed in several other systems around the first order magnetic transition with reduction of magnetization during cooling [8–12]. In this paper, we report the IMCE in $Ni_{1.68}Co_{0.32}Mn_{1.20}Ga_{0.80}$ alloy, in which structural transformation is accompanied with a large metamagnetic transition below T_c ($T_M < T_c$). The observation of exchange bias (EB) effect confirms the coexistence of AFM and FM phases in the martensitic state.

2. Results and Discussion

Figure 1a shows the temperature dependence of magnetization M(T) measured at H = 100 Oe under zero-field-cooled (ZFC), field-cooled cooling (FCC) and field-cooled heating (FCH) modes, respectively. At high temperatures, in the austenitic state, the sample is paramagnetic and orders ferromagnetically below T_c = 429 K (inset of Figure 1a). However, as the temperature further decreases, a sudden drop in magnetization takes place at about 228 K as a result of the MT and entered a steady state with a lower magnetization. The thermal hysteresis observed between the FCC and FCH processes across the MT confirms the first order nature of this transition. The behavior of the magnetization of martensitic state depends strongly on the thermomagnetic history of the sample. The M(T) curves measured under 20 and 60 kOe fields are similar to that of 100 Oe, showing a large ΔM between austenite and martensite. MT temperatures decrease with increasing magnetic field, e.g., the T_M is decreased by about 23 K with the application of 60 kOe field (inset of Figure 1b). This shows that the magnetic field can induce reverse MT from martensite to austenite in the Co and Mn co-doped Ni_2MnGa alloy which is further confirmed by the resistivity measurement and shows a giant magnetoresistance effect [13].

As we know, the ΔM of Ni_2MnGa across the MT is very small due to the fact that both martensitic and austenitic states are FM. However, in the Mn-doped Ni_2MnGa alloy, the extra Mn atoms which occupy the Ga sites reduce the distance between Mn atoms, leading to the magnetic moments partially align antiferromagnetically in both martensite and austenite [14]. On the other hand, the partial substitution of Ni by Co in Mn-doped Ni_2MnGa can further change the magnetic ordering in the austenitic state from antiferromagnetic (AFM) to FM [15]. As a result, the Co and Mn co-doping produces a competition between AFM and FM, which is similar to the state in the Co and Fe co-doped Ni_2MnGa alloys [12]. Extended X-ray Absorption Fine Structure (EXAFS) results show that the distance of Mn atoms decreases across MT from austenite to martensite [16]. The decrease of the Mn-Mn distance between 4(*a*) and 4(*b*) sites (4(*a*) and 4(*b*) sites are the Mn and Ga sites in the stoichiometric compound, respectively) may introduce AFM exchange, forming partial AFM in the FM matrix, *i.e.*, coexistence of FM and AFM in martensite in the present alloy. One way to clarify this

point is to study the EB effect of the sample, which has been used successfully in NiMn-based alloys [17–21].

Figure 1. (**a**) zero-field-cooled (ZFC), field-cooled cooling (FCC), and field-cooled heating (FCH) M(T) of the sample measured under H = 100 Oe. The inset shows the temperature dependence of the ac susceptibility ($\chi(T)$) at higher temperatures intended to obtain the T_c. (**b**) M(T) of the sample under high magnetic fields in FCC and FCH conditions respectively. The inset shows the field dependence of MT starting temperature ($T_M(H)$). The T_M temperatures under different fields are indicated by arrows.

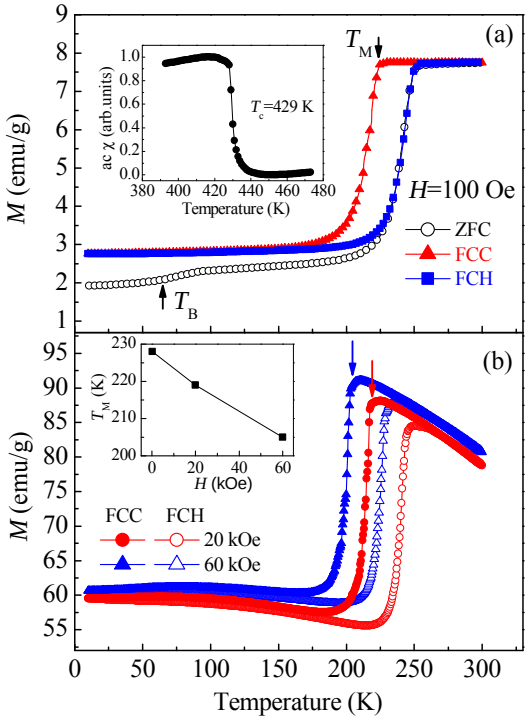

It is well known that when a sample with FM/AFM interfaces is cooled under magnetic field, the hysteresis loop is shifted along the field axis (called EB) below blocking temperature (T_B) [19,22]. In order to confirm the coexistence of AFM and FM, we measured the hysteresis loops of magnetizations from −20 kOe to 20 kOe at 10 K after ZFC and FCC (H = 10 kOe) from 300 K, respectively. For clear visualization of the loops shift, only the loops form −1 to 1 kOe are shown in Figure 2a. The ZFC loop is symmetrical around zero point, whereas the shift of the FCC loops towards negative field provides evidence on the existence of EB. Moreover, the coercivity (H_c) of FCC loop (99.5 Oe) is higher than that of ZFC loop (61.5 Oe), which is ascribed to the development of the exchange anisotropy after FCC [22]. Figure 2b shows the EB field (H_{EB}) and H_c as a function of temperature. The H_{EB} and H_c are defined as $H_{EB} = -(H_1 + H_2)/2$ and $H_c = -(H_1 - H_2)/2$, respectively. Here, H_1 and H_2 are the left and right coercive fields, respectively. The H_{EB} approximately linearly decreases with increasing temperature in the low temperature regions and gradually disappears around T_B. The T_B can also be identified from ZFC M(T) curve (Figure 1a). The magnetization increases at T_B indicating the AFM can no longer pin the FM domain. With the anisotropy of AFM deceasing with increasing temperature, the FM rotation can drag more AFM spins, giving rise to the increase in H_c; whereas the AFM no

longer hinders the FM rotation above T_B. As a result, the H_c reaches its maximum value and H_{EB} reduces to zero at higher temperatures. This further confirms that some AFM exchange occurs inside the FM matrix in the martensite.

Figure 2. (**a**) Hysteresis loops of magnetization at 10 K after ZFC and FCC (H = 10 kOe) from 300 K. (**b**) EB field (H_{EB}) and coercivity (H_c) as a function of temperature.

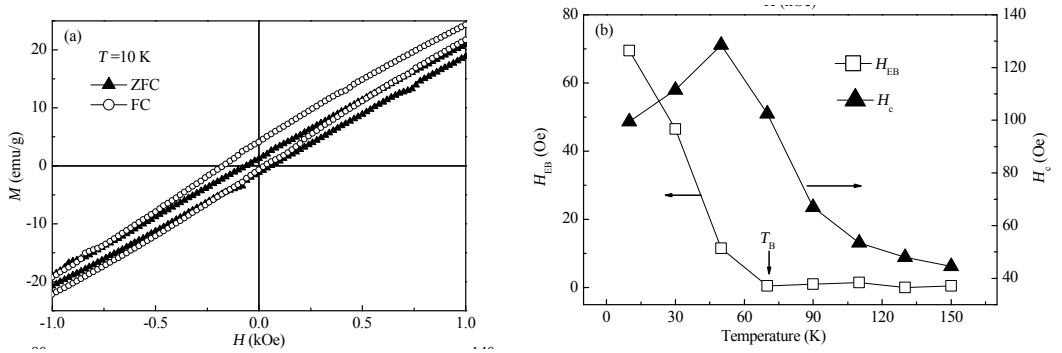

The IMCE can be expected within the MT temperature range in Co and Mn co-doped Ni_2MnGa alloy due to the reduction of magnetization during the MT resulting from the formation of partially AFM phase. In order to determine the magnetic entropy change (ΔS_M) across the MT, we measured the isothermal magnetization M(H) curves of $Ni_{1.68}Co_{0.32}Mn_{1.20}Ga_{0.80}$. Magnetic field up to 60 kOe was applied isothermally between 210 and 252 K. In Figure 3, only a portion of the curves within the transformation temperature range is shown for clarity. The typical metamagnetic behavior due to the field-induced reverse MT is observed between 222 and 238 K. Above 240 K, the magnetization curves exhibit characteristics of a ferromagnet. Similarly, the metamagnetic behavior disappears below 220 K, giving rise to a FM behavior with lower saturation magnetization than that of high-temperature phase. The ΔS_M can be calculated from magnetization isotherms using the Maxwell relation:

$$\Delta S_M = \int_0^H \left(\frac{\partial M}{\partial T} \right)_H dH \tag{1}$$

For magnetization measurements made at discrete temperatures and field intervals, the ΔS_M can be approximated by:

$$\Delta S_M \approx \frac{1}{\Delta T} \left[\int_0^H M(T + \Delta T) dH - \int_0^H M(T) dH \right] \tag{2}$$

For a truly discontinuous first order phase transition, since the $[\partial M/\partial T]_H$ does not exist theoretically, Equations 1 and 2 cannot be used to calculate the ΔS_M. But in reality, the first order phase transition is not ideal and the change of magnetization occurs over a few Kelvin temperature range, as a result, the $[\partial M/\partial T]_H$ can be measured experimentally [23].

Figure 3. Isothermal M(H) of $Ni_{1.68}Co_{0.32}Mn_{1.20}Ga_{0.80}$ around the MT temperature range. The arrows indicate the direction of change of the applied field, and the shaded area represents the hysteretic loss for T = 228 K isotherm. The inset shows the hysteretic loss as a function of temperature.

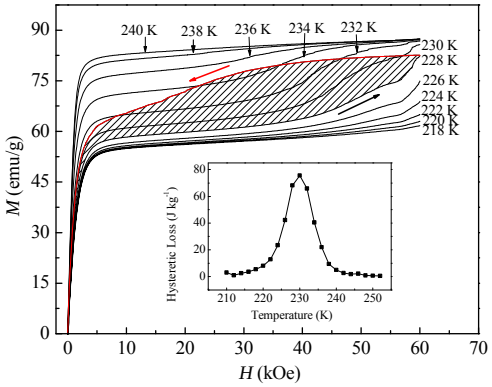

The temperature dependencies of the ΔS_M under different magnetic fields are shown in Figure 4. The most striking features of the ΔS_M are the large and positive entropy change within the MT temperature range. The positive sign of ΔS_M exists even under high magnetic field, showing the mechanism involved is different from that of Co-free Ni-Mn-Ga alloys which is related to the coupling between the martensitic and magnetic domains [4]. The modification of magnetic order through magnetic-field-induced reverse MT from partially AFM martensite to FM austenite is responsible for the IMCE in the present alloy. The ΔS_M^{max} increases with ΔH and shows saturation for lager ΔH (inset of Figure 4). The saturation of the ΔS_M^{max} as a function of the field and the broadening of ΔS_M (T) with increasing field are characteristic features of first order magnetic transition [7]. The ΔS_M is 16.2 J Kg^{-1} K^{-1} for ΔH = 60 kOe field. Compared with other IMCE materials, the ΔS_M for ΔH = 60 kOe in the present alloy is comparable to the value observed in Ni-Mn-Sn alloys [10], and is two times larger than the value observed in $Mn_{1.95}Cr_{0.05}Sb$ [8]. One important parameter to evaluate the magnetocaloric properties of a given material is the refrigeration capacity (RC), giving the amount of heat that can be transferred in one thermodynamic cycle. The RC is usually calculated by integrating the ΔS_M (T) curve over the full width at half maximum (the shaded area in Figure 4), which yields a value of about 125 J kg^{-1} for ΔH = 60 kOe. For a first order magnetic phase transition, the hysteretic loss is another key parameter for evaluating the MCE around transition, which is equal to the area between the increasing and decreasing magnetic field segments of the magnetization curves (the shaded area in Figure 3). The hysteretic loss as a function of the temperature is shown in the inset of Figure 2, giving a maximum at almost the same temperature as the maximum of the ΔS_M (T) curve. The average hysteretic loss over the same temperature range as that of RC is about 57 J kg^{-1}. Thus, the net RC is 68 J kg^{-1} obtained by subtracting the average hysteretic loss from the RC. This value is comparable to the maximum value obtained by Cu doping in Ni_2MnGa alloys, but with opposite sign in ΔS_M [6]. Note that the high value of the ΔS_M alone is not enough to evaluate the MCE of a material. Another important parameter for MCE is adiabatic temperature change (ΔT_{ad}), which can be measured directly in adiabatic system with application of a magnetic field [7,11,24] or be estimated from the magnetization and specific heat measurements [25]. Thus, some further studies, such as the measurement of ΔT_{ad}, are needed to further evaluate the IMCE in the present alloy.

Figure 4. Temperature dependence of the ΔS_M under different magnetic field variations (ΔH). The shaded area indicates the RC at ΔH = 60 kOe. The inset shows the field dependence of maximum ΔS_M within the MT temperature range at T = 232 K.

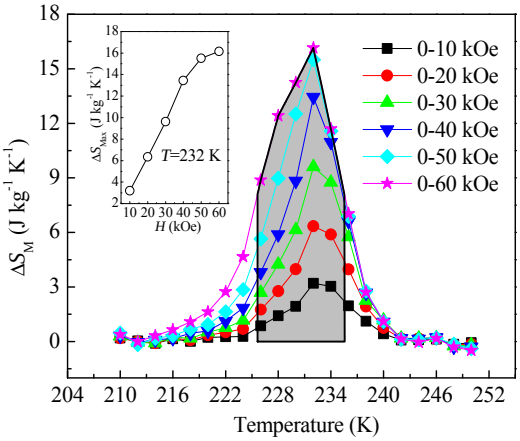

3. Experimental Section

A polycrystalline $Ni_{1.68}Co_{0.32}Mn_{1.20}Ga_{0.80}$ alloy was prepared with an arc-melting technique under argon atmosphere using Ni, Co, Mn, and Ga of 99.9% purity. The sample was remelted several times and subsequently annealed at 1000 °C for 24 h before being slowly cooled to room temperature to ensure homogeneity. The composition was determined by energy dispersive X-ray analysis (EDX) (Figure 5). The ac susceptibility measurement was performed to determine the T_c. The magnetization measurements were performed on a physical properties measurement system (Quantum Design) platform with a vibrating sample magnetometer module.

Figure 5. EDX spectrum of $Ni_{1.68}Co_{0.32}Mn_{1.20}Ga_{0.80}$. The inset shows the scanning electron microscopic image. The little rectangle marks the position at which the EDX spectrum was taken.

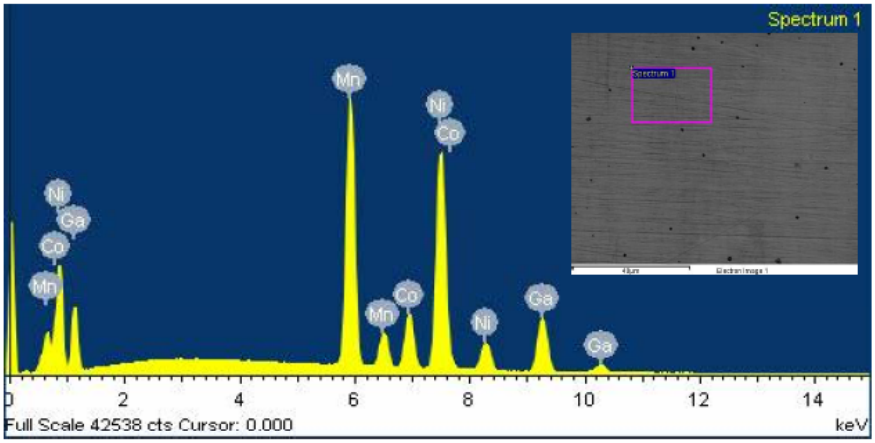

4. Conclusions

In conclusion, a large positive ΔS_M has been found in Mn and Co co-doped Ni_2MnGa alloy within the MT temperature range. The partial substitution of Ni by Co in Mn-doped Ni_2MnGa, a typical

partially AFM material, modifies the exchange interaction among Mn atoms and results in a change from AFM to FM in the austenite. The modification of magnetic order from partially AFM martensite to FM austenite through magnetic-field-induced reverse MT is responsible for the IMCE in the present alloy. The observation of EB effect confirms that some AFM exchange exists inside the FM matrix of martensite. The IMCE with a high net RC indicates that the present alloy may be a promising candidate for magnetic refrigeration.

Conflict of Interest

The authors declare no conflict of interest.

References

1. Vasil'ev, A.N.; Bozhko, A.D.; Khovailo, V.V.; Dikshtein, I.E.; Shavrov, V.G.; Buchelnikov, V.D.; Matsumoto, M.; Suzuki, S.; Takagi, T.; Tani, J. Structural and magnetic phase transitions in shape-memory alloys $Ni_{2+x}Mn_{1-x}Ga$. *Phys. Rev. B* **1999**, *59*, 1113–1120.
2. Hu, F.X.; Shen, B.G.; Sun, J.R. Magnetic entropy change in $Ni_{51.5}Mn_{22.7}Ga_{25.8}$ alloy. *Appl. Phys. Lett.* **2000**, *76*, 3460–3463.
3. Pareti, L.; Solzi, M.; Albertini, F.; Paoluzi, A. Giant entropy change at the co-occurrence of structural and magnetic transitions in the $Ni_{2.19}Mn_{0.81}Ga$ Heusler alloy. *Eur. Phys. J. B* **2003**, *32*, 303–307.
4. Marcos, J.; Mañosa, L.; Planes, A.; Casanova, F.; Batlle, X.; Labarta, A. Multiscale origin of the magnetocaloric effect in Ni-Mn-Ga shape-memory alloys. *Phys. Rev. B* **2003**, *68*, 094401:1–094404:6.
5. Pasquale, M.; Sasso, C.P.; Lewis, L.H.; Giudici, L.; Lograsso, T.; Schlagel, D. Magnetostructural transition and magnetocaloric effect in $Ni_{55}Mn_{20}Ga_{25}$ single crystals. *Phys. Rev. B* **2005**, *72*, doi:10.1103/PhysRevB.72.094435.
6. Stadler, S.; Khan, M.; Mitchell, J.; Ali, N.; Gomes, A.M.; Dubenko, I.; Takeuchi, A.Y.; Guimaraes, A.P. Magnetocaloric properties of $Ni_2Mn_{1-x}Cu_xGa$. *Appl. Phys. Lett.* **2006**, *88*, 192511:1–192511:3.
7. Giguère, A.; Foldeaki, M.; Ravi Gopal, B.; Chahine, R.; Bose, T.K.; Frydman, A.; Barclay, J.A. Direct measurement of the "giant" adiabatic temperature change in $Gd_5Si_2Ge_2$. *Phys. Rev. Lett.* **1999**, *83*, 2262–2265.
8. Tegus, O.; Bruck, E.; Zhang, L.; Dagula; Buschow, K.H.J.; de Boer, F.R. Magnetic-phase transitions and magnetocaloric effects. *Physica B* **2002**, *319*, 174–192.
9. Han, Z.D.; Wang, D.H.; Zhang, C.L.; Tang, S.L.; Gu, B.X.; Du, Y.W. Large magnetic entropy changes in the $Ni_{45.4}Mn_{41.5}In_{13.1}$ ferromagnetic shape memory alloy. *Appl. Phys. Lett.* **2006**, *89*, 182507:1–182507:3.
10. Krenke, T.; Duman, E.; Acet, M.; Wassermann, E.F.; Moya, X.; Mañosa, L.; Planes, A. Inverse magnetocaloric effect in ferromagnetic Ni-Mn-Sn alloys. *Nat. Mater.* **2005**, *4*, 450–454.
11. Moya, X.; Mañosa, L.; Planes, A.; Aksoy, S.; Acet, M.; Wassermann, E.F.; Krenke, T. Cooling and heating by adiabatic magnetization in the $Ni_{50}Mn_{34}In_{16}$ magnetic shape-memory alloy. *Phys. Rev. B* **2007**, *75*, 184412:1–184412:5.

12. Pathak, A.K.; Dubenko, I.; Karaca, H.E.; Stadler, S.; Ali, N. Large inverse magnetic entropy changes and magnetoresistance in the vicinity of a field-induced martensitic transformation in $Ni_{50-x}Co_xMn_{32-y}Fe_yGa_{18}$. *Appl. Phys. Lett.* **2010**, *97*, 062505:1–062505:3.
13. Wang, B.M.; Ren, P.; Liu, Y.; Wang, L. Enhanced magnetoresistance through magnetic-field-induced phase transition in Ni_2MnGa co-doped with Co and Mn. *J. Magn. Magn. Mater.* **2010**, *322*, 715–717.
14. Enkovaara, J.; Heczko, O.; Ayuela, A.; Nieminen, R.M. Coexistence of ferromagnetic and antiferromagnetic order in Mn-doped Ni_2MnGa. *Phys. Rev. B* **2003**, *67*, 212405:1–212405:4.
15. Yu, S.Y.; Cao, Z.X.; Ma, L.; Liu, G.D.; Chen, J.L.; Wu, G.H.; Zhang, B.; Zhang, X.X. Realization of magnetic field-induced reversible martensitic transformation in NiCoMnGa alloys. *Appl. Phys. Lett.* **2007**, *91*, 102507:1–102507:3.
16. Bhobe, P.A.; Priolkar, K.R.; Sarode, P.R. Factors influencing the martensitic transformation in $Ni_{50}Mn_{35}Sn_{15}$: An EXAFS study. *J. Phys. Condens. Mater.* **2008**, *20*, doi:10.1088/0953-8984/20/01/015219.
17. Khan, M.; Dubenko, I.; Stadler, S.; Ali, N. Exchange bias in bulk Mn rich Ni-Mn-Sn Heusler alloys. *J. Appl. Phys.* **2007**, *102*, 113914:1–113914:4.
18. Pathak, A.K.; Khan, M.; Gautam, B.R.; Stadler, S.; Dubenko, I.; Ali, N. Exchange bias in bulk Ni-Mn-In-based Heusler alloys. *J. Magn. Magn. Mater.* **2009**, *321*, 963–965.
19. Wang, B.M.; Liu, Y.; Wang, L.; Huang, S.L.; Zhao, Y.; Yang, Y.; Zhang, H. Exchange bias and its training effect in the martensitic state of bulk polycrystalline $Ni_{49.5}Mn_{34.5}In_{16}$. *J. Appl. Phys.* **2008**, *104*, 043916:1–043916:4.
20. Wang, B.M.; Liu, Y.; Xia, B.; Ren, P.; Wang, L. Large exchange bias obtainable through zero-field cooling from an unmagnetized state in Ni-Mn-Sn alloys. *J. Appl. Phys.* **2012**, *111*, 043912:1–043912:7.
21. Wang, B.M.; Liu, Y.; Ren, P.; Xia, B.; Ruan, K.B.; Yi, J.B.; Ding, J.; Li, X.G.; Wang, L. Large exchange bias after zero-field cooling from an unmagnetized state. *Phys. Rev. Lett.* **2011**, *106*, 077203:1–077203:4.
22. Nogués, J.; Schuller, I.K. Exchange bias. *J. Magn. Magn. Mater.* **1999**, *192*, 203–232.
23. Gschneidner, K.A., Jr.; Pecharsky, V.K.; Tsokol, A.O. Recent developments in magnetocaloric materials. *Rep. Prog. Phys.* **2005**, *68*, doi:10.1088/0034-4885/68/6/R04.
24. Khovaylo, V.V.; Skokov, K.P.; Koshkid'ko, Y.S.; Koledov, V.V.; Shavrov, V.G.; Buchelnikov, V.D.; Taskaev, S.V.; Miki, H.; Takagi, T.; Vasiliev, A.N. Adiabatic temperature change at first-order magnetic phase transitions: $Ni_{2.19}Mn_{0.81}Ga$ as a case study. *Phys. Rev. B* **2008**, *78*, 060403:1–060403:4.
25. Pecharsky, V.K.; Gschneidner, K.A., Jr. Giant magnetocaloric effect in $Gd_5(Si_2Ge_2)$. *Phys. Rev. Lett.* **1997**, *78*, 4494–4497.

© 2013 by the authors; licensee MDPI, Basel, Switzerland. This article is an open access article distributed under the terms and conditions of the Creative Commons Attribution license (http://creativecommons.org/licenses/by/3.0/).